The Astrophysical Journal, 721:90–97, 2010 September 20 doi:10.1088/0004-637X/721/1/90

SPT-CL J0546-5345: A MASSIVE $z > 1$ GALAXY CLUSTER SELECTED VIA THE SUNYAEV–ZEL'DOVICH EFFECT WITH THE SOUTH POLE TELESCOPE

M. Brodwin[1,25,26], J. Ruel[2], P. A. R. Ade[3], K. A. Aird[4], K. Andersson[5], M. L. N. Ashby[1], M. Bautz[5], G. Bazin[6,7], B. A. Benson[8,9], L. E. Bleem[8,10], J. E. Carlstrom[8,9,10,11], C. L. Chang[8,9], T. M. Crawford[8,11], A. T. Crites[8,11], T. de Haan[12], S. Desai[13], M. A. Dobbs[12], J. P. Dudley[12], G. G. Fazio[1], R. J. Foley[1,27], W. R. Forman[1], G. Garmire[14], E. M. George[15], M. D. Gladders[8,11], A. H. Gonzalez[16], N. W. Halverson[17], F. W. High[2], G. P. Holder[12], W. L. Holzapfel[15], J. D. Hrubes[4], C. Jones[1], M. Joy[18], R. Keisler[8,10], L. Knox[19], A. T. Lee[15,20], E. M. Leitch[8,11], M. Lueker[15], D. P. Marrone[4,8], J. J. McMahon[8,9,21], J. Mehl[8,11], S. S. Meyer[8,9,10,11], J. J. Mohr[6,7,22,26], T. E. Montroy[23], S. S. Murray[1], S. Padin[8,11], T. Plagge[11,15], C. Pryke[8,9,11], C. L. Reichardt[15], A. Rest[2], J. E. Ruhl[23], K. K. Schaffer[8,9], L. Shaw[12,24], E. Shirokoff[15], J. Song[13], H. G. Spieler[20], B. Stalder[1], S. A. Stanford[19], Z. Staniszewski[23], A. A. Stark[1], C. W. Stubbs[1,2], K. Vanderlinde[12], J. D. Vieira[8,10], A. Vikhlinin[1], R. Williamson[8,11], Y. Yang[13], O. Zahn[15], and A. Zenteno[6,7]

[1] Harvard-Smithsonian Center for Astrophysics, 60 Garden Street, Cambridge, MA 02138, USA
[2] Department of Physics, Harvard University, 17 Oxford Street, Cambridge, MA 02138, USA
[3] Department of Physics and Astronomy, Cardiff University, CF24 3YB, UK
[4] University of Chicago, 5640 South Ellis Avenue, Chicago, IL 60637, USA
[5] Kavli Institute for Astrophysics and Space Research, MIT, Cambridge, MA 02139, USA
[6] Department of Physics, Ludwig-Maximilians-Universität, Scheinerstr. 1, 81679 München, Germany
[7] Excellence Cluster Universe, Boltzmannstr. 2, 85748 Garching, Germany
[8] Kavli Institute for Cosmological Physics, University of Chicago, 5640 South Ellis Avenue, Chicago, IL 60637, USA
[9] Enrico Fermi Institute, University of Chicago, 5640 South Ellis Avenue, Chicago, IL 60637, USA
[10] Department of Physics, University of Chicago, 5640 South Ellis Avenue, Chicago, IL 60637, USA
[11] Department of Astronomy and Astrophysics, University of Chicago, 5640 South Ellis Avenue, Chicago, IL 60637, USA
[12] Department of Physics, McGill University, 3600 Rue University, Montreal, Quebec H3A 2T8, Canada
[13] Department of Astronomy, University of Illinois, 1002 West Green Street, Urbana, IL 61801, USA
[14] Department of Astronomy and Astrophysics, Pennsylvania State University, 525 Davey Lab, University Park, PA 16802, USA
[15] Department of Physics, University of California, Berkeley, CA 94720, USA
[16] Department of Astronomy, University of Florida, Gainesville, FL 32611, USA
[17] Department of Astrophysical and Planetary Sciences and Department of Physics, University of Colorado, Boulder, CO 80309, USA
[18] Department of Space Science, VP62, NASA Marshall Space Flight Center, Huntsville, AL 35812, USA
[19] Department of Physics, University of California, One Shields Avenue, Davis, CA 95616, USA
[20] Physics Division, Lawrence Berkeley National Laboratory, Berkeley, CA 94720, USA
[21] Department of Physics, University of Michigan, 450 Church Street, Ann Arbor, MI, 48109, USA
[22] Max-Planck-Institut für extraterrestrische Physik, Giessenbachstr. 85748 Garching, Germany
[23] Physics Department and CERCA, Case Western Reserve University, 10900 Euclid Ave., Cleveland, OH 44106, USA
[24] Department of Physics, Yale University, P.O. Box 208210, New Haven, CT 06520-8120, USA

Received 2010 July 12; accepted 2010 July 24; published 2010 August 26

ABSTRACT

We report the spectroscopic confirmation of SPT-CL J0546-5345 at $\langle z \rangle = 1.067$. To date this is the most distant cluster to be spectroscopically confirmed from the 2008 South Pole Telescope (SPT) catalog, and indeed the first $z > 1$ cluster discovered by the Sunyaev–Zel'dovich Effect (SZE). We identify 21 secure spectroscopic members within 0.9 Mpc of the SPT cluster position, 18 of which are quiescent, early-type galaxies. From these quiescent galaxies we obtain a velocity dispersion of 1179^{+232}_{-167} km s^{-1}, ranking SPT-CL J0546-5345 as the most dynamically massive cluster yet discovered at $z > 1$. Assuming that SPT-CL J0546-5345 is virialized, this implies a dynamical mass of $M_{200} = 1.0^{+0.6}_{-0.4} \times 10^{15}\, M_\odot$, in agreement with the X-ray and SZE mass measurements. Combining masses from several independent measures leads to a best-estimate mass of $M_{200} = (7.95 \pm 0.92) \times 10^{14}\, M_\odot$. The spectroscopic confirmation of SPT-CL J0546-5345, discovered in the wide-angle, mass-selected SPT cluster survey, marks the onset of the high-redshift SZE-selected galaxy cluster era.

Key words: galaxies: clusters: individual (SPT-CL J0546-5345) – galaxies: distances and redshifts – galaxies: evolution

Online-only material: color figure

1. INTRODUCTION

Formed from the extreme peaks of the primordial density field, galaxy clusters are both a sensitive probe of cosmology and an excellent laboratory for galaxy evolution studies. Although massive galaxy clusters are easy to identify in the local universe, finding such objects at large lookback times has been extremely challenging. A patchwork of optical, infrared, and X-ray techniques has led to a heterogeneous sample of distant galaxy clusters (e.g., Stanford et al. 1997; Rosati et al. 2004; Gladders & Yee 2005; Mullis et al. 2005; Brodwin et al. 2006; Elston et al. 2006; Stanford et al. 2006; Eisenhardt et al. 2008; Muzzin et al. 2009; Papovich et al. 2010). While each technique

[25] W. M. Keck Postdoctoral Fellow at the Harvard-Smithsonian Center for Astrophysics
[26] Visiting astronomer, Cerro Tololo Inter-American Observatory, National Optical Astronomy Observatory, under contract with the National Science Foundation
[27] Clay Fellow

offers unique advantages, namely, observational efficiency (optical), redshift reach and mass sensitivity (IR), and a direct mass observable (X-ray), none produce purely mass-selected, nearly redshift independent cluster samples.

A long-awaited advance is the arrival of Sunyaev–Zel'dovich Effect (SZE) cluster surveys. The SZE is a small distortion in the cosmic microwave background (CMB) spectrum caused by the inverse Compton scattering of CMB photons with the hot intracluster medium (ICM; Sunyaev & Zel'dovich 1972). The surface brightness of the SZE does not depend on a cluster's distance, which makes it a nearly redshift-independent method for finding massive galaxy clusters (e.g., Carlstrom et al. 2002). A new generation of dedicated millimeter-wave (mm-wave) experiments to search for galaxy clusters are currently surveying large areas of sky, including the Atacama Cosmology Telescope (Fowler et al. 2007) and the South Pole Telescope (SPT; Carlstrom et al. 2009).

Taking advantage of the excellent conditions for mm-wave observations at the South Pole, the 10 m SPT (Carlstrom et al. 2009) is midway through a $\gtrsim$2000 deg^2 survey sensitive to galaxy clusters above $\approx 5 \times 10^{14}\, M_\odot$ at all redshifts. The first three clusters discovered by the SZE were reported by Staniszewski et al. (2009, hereafter S09). The complete 5σ cluster catalog from the 2008 SPT season, a study of the optical properties of these clusters, and a description of the survey strategy and goals are given in Vanderlinde et al. (2010, hereafter V10) and High et al. (2010, hereafter H10).

Here we report the spectroscopic confirmation, velocity dispersion, and dynamical mass of the first $z > 1$ SZE-selected cluster, SPT-CL J0546-5345, at $\langle z \rangle = 1.067$. In converting from r_{500} to r_{200} and M_{500} to M_{200} throughout, we assume a Navarro–Frenk–White (NFW) density profile and the mass-concentration relation of Duffy et al. (2008). Unless otherwise indicated, we use Vega magnitudes and adopt a WMAP5 cosmology (Dunkley et al. 2009), with $\Omega_M = 0.264$, $\Omega_\Lambda = 0.736$, $\sigma_8 = 0.80$, and $H_0 = 71$ km s^{-1} Mpc^{-1}.

2. OBSERVATIONS

2.1. SPT-SZE

In 2008, the SPT survey observed a 196 deg^2 area (178 deg^2 after point-source and non-uniform coverage masking) for $\sim$1500 hr (V10), reaching a 5σ point source sensitivity of $\sim$7 mJy at 150 GHz (2.0 mm). Details of the data processing, map-making, cluster extraction, and significance estimates are given in S09 and V10. SPT-CL J0546-5345, first reported in S09, has an SZE decrement of S/N = 7.69 at 150 GHz. It is among the most significant of the 2008 cluster candidates with a $z \gtrsim 1$ optical red sequence (H10). SZE significance contours at 150 GHz are shown in Figure 1 (left).

2.2. Spitzer/IRAC and Optical Imaging

Mid-infrared *Spitzer*/Infrared Array Camera (IRAC) imaging was obtained in 2009 September as part of a larger program to follow up clusters identified in the SPT survey (PID 60099; PI Brodwin). The on-target observations consisted of 8×100 s and 6×30 s dithered exposures at 3.6 and 4.5 μm, respectively. The deep 3.6 μm observations are sensitive to passively evolving cluster galaxies down to 0.1 L^* at $z = 1.5$. The data were reduced following the method of Ashby et al. (2009). Briefly, we correct for column pulldown, mosaic the individual exposures, resample to 0.″86 pixels (half the solid angle of the native IRAC pixels), and reject cosmic rays.

Optical data were provided by the Blanco Cosmology Survey (BCS), an NOAO survey program with deep $griz$ imaging over 100 deg^2 in a subset of the SPT 05 hr and 23 hr fields (Ngeow et al. 2009). The Stellar Locus Regression method of High et al. (2009) was used for photometric calibration, extinction correction, and Galactic de-reddening. The independent calibration from the DES data management system (Mohr et al. 2008) gave consistent results. The BCS data typically reach 5σ AB depths of 24.75, 24.65, 24.35, and 23.5 in $griz$. See S09 and H10 for a more detailed description of the optical data.

Along with the r and i BCS photometry, the IRAC 3.6 μm data were used to select promising cluster member candidates for spectroscopy as described below. A false-color optical (ri) + IRAC (3.6 μm) image is shown in Figure 1 (right). The optical-only (grz) image (Figure 1, left) indicates how optically (rest-frame UV) faint the cluster members are, and highlights the importance of *Spitzer*/IRAC imaging for high-redshift cluster detection and study.

2.3. Chandra

SPT-CL J0546-5345 was observed with *Chandra*/ACIS-I on four separate occasions, for a total exposure time of 55.6 ks (PID 09800046; PI Garmire, PID 11800471; PI Mohr). This yielded 1304 source counts in the 0.5–7.0 keV energy range within $0.5\, r_{500}$. Background was subtracted using blank sky data normalized to the flux in the 9.5–12 keV energy band. The cluster luminosity is $L_X(0.5\text{–}2\,\mathrm{keV}) = (6.4 \pm 0.4) \times 10^{44}$ erg s^{-1}, and the temperature, estimated in the $(0.15\text{–}1)\, r_{500}$ annulus, is $T_X = 7.5^{+1.7}_{-1.1}$ keV. The gas mass was estimated to be $M_{g,500} = 7.3^{+0.4}_{-0.3} \times 10^{13}\, M_\odot$ from the X-ray surface brightness in the 0.5–2.0 keV band following the analysis method described in Vikhlinin et al. (2006), where the gas density is assumed to follow a modified β-model (Cavaliere & Fusco-Femiano 1978) that is allowed to steepen at large radii and to have a power-law cusp at the cluster center. The *Chandra* X-ray contours are overlaid in Figure 1 (right). The reader is referred to Andersson et al. (2010, hereafter A10) for a full description of the X-ray analysis of SPT-CL J0546-5345, as well as a study of the X-ray properties of 15 of the SZE-selected clusters from the V10 sample.

2.4. Optical Spectroscopy

Multislit spectroscopic observations were acquired on the 6.5 meter Magellan Baade telescope on UT 2010 February 11. We used the Gladders Image-Slicing Multi-Slit Option (GISMO[28]; M. D. Gladders et al. 2010, in preparation) module on the Inamori Magellan Areal Camera and Spectrograph (IMACS; Dressler et al. 2006). GISMO optically remaps the central region of the IMACS field of view (roughly 3.′5 × 3.′2) to 16 evenly spaced regions of the focal plane, allowing for a large density of slitlets in the cluster core while minimizing trace overlaps on the CCD. We used the f/2 camera for its greater red sensitivity, the 300 l/mm "red" grism, and the WB6300-9500 filter. The seeing was excellent ($\lesssim$0.″5) throughout the six 30 minute exposures.

In designing the multislit mask, galaxies were assigned a weight proportional to their i-band brightness and their proximity to the cluster center, and inversely proportional to their distance in color space, in both $r - i$ and $i - [3.6]$, from the predicted color from a Bruzual & Charlot (2003, hereafter

[28] http://www.lco.cl/telescopes-information/magellan/instruments/imacs/gismo

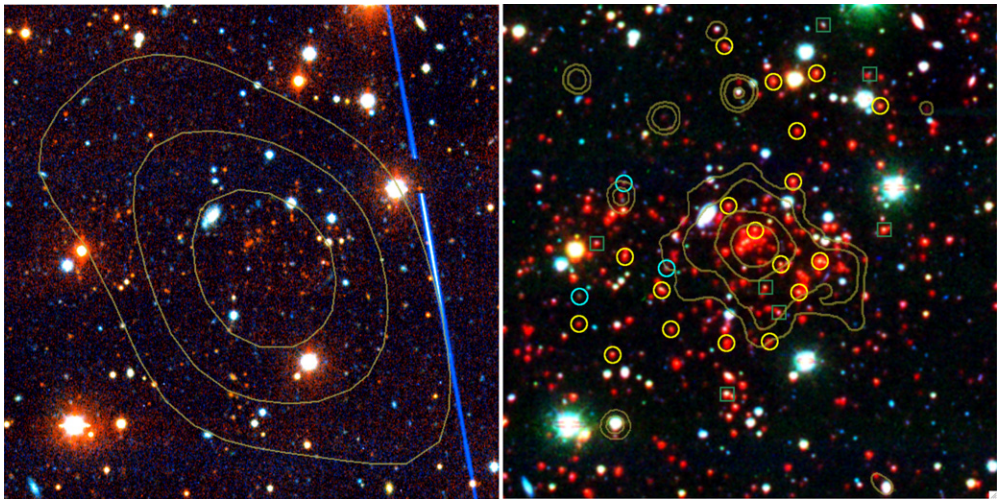

Figure 1. Left: optical $4' \times 4'$ color image (grz) of SPT-CL J0546-5345, with SZE significance contours overlaid (S/N = 2, 4, and 6). Right: false color optical (ri)+IRAC (3.6 μm) image of SPT-CL J0546-5345, with *Chandra* X-ray contours overlaid (0.25, 0.4, 0.85, and 1.6 counts per $2'' \times 2''$ pixel per 55.6 ks in the 0.5–2 keV band). North is up, east is to the left. Due to its high angular resolution, *Chandra* is able to resolve substructure to the SW, which may be evidence of a possible merger. These images highlight the importance of IRAC imaging in studying the galaxies in high-redshift, optically faint clusters. Spectroscopic early-type (late-type) members are indicated with yellow (cyan) circles. Green squares show the spectroscopic non-members.

BC03) passively evolving 100 Myr burst model with formation redshift $z_f = 3$.

The COSMOS reduction package[29] was used for standard CCD processing, resulting in wavelength-calibrated two-dimensional spectra. The one-dimensional spectra were then extracted from the sum of the reduced data. We flux calibrated the data and removed telluric absorption using the continuum of a spectrophotometric standard (Foley et al. 2003).

3. RESULTS

3.1. Redshifts

Redshifts for galaxy spectra exhibiting significant absorption features were found through cross-correlation using the RVSAO package in IRAF[30] (Kurtz & Mink 1998). The validity of the cross-correlation redshift was checked by visual inspection and judged by the presence of visible absorption lines; most of these displayed clear Ca HK lines. For three members the redshift was determined from a strong, unresolved [O II] emission line. Redshift uncertainties were estimated as twice those given by RVSAO (Quintana et al. 2000). An independent extraction and visual redshift determination yielded identical redshifts for all cluster members within the errors.

From these Magellan observations we obtained 28 secure redshifts, of which 21 are spectroscopic cluster members within $r < 0.9$ Mpc of the SPT cluster position. This high success rate validates our spectroscopic selection algorithm. Representative spectra are shown in Figure 2. The majority of the members (18) are quiescent, with redshifts determined from Ca HK absorption, as expected given their red-sequence selection, central location, and the extreme mass of the cluster.

3.2. Velocity Dispersion

An iterative 3σ clipping algorithm was used to identify cluster members. We list the 21 secure cluster members in Table 1, and plot the redshift histogram in Figure 3 (left). In this figure the 18 passive members, for which the redshift was obtained from Ca HK absorption lines, are shaded red. Redshifts of the remaining three members, shaded blue, were secured from strong [O II] emission. Spectroscopic non-members are unshaded. From the spectroscopic redshift histogram, SPT-CL J0546-5345 appears to be a single massive halo, with no evidence of substructure or merger activity. We note, however, that the X-ray image (Figure 1) shows a substructure extending to the SW indicating that a minor merger may be taking place (A10).

We use the robust biweight estimator of Beers et al. (1990) to estimate the mean velocity and velocity dispersion, applying the relativistic correction and the usual correction for velocity

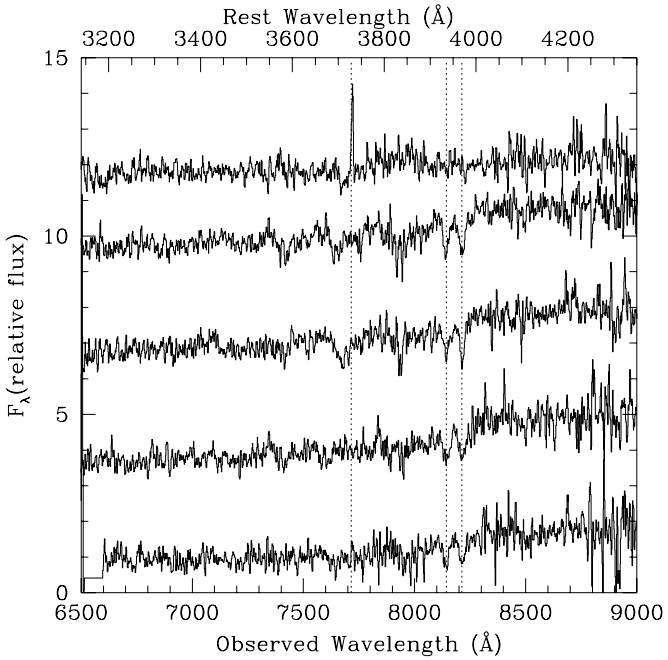

Figure 2. Representative spectra of cluster member galaxies for SPT-CL J0546-5345. Vertical dotted lines indicate [O II] and Ca HK features. Most (18/21) confirmed members are passive, early-type galaxies.

[29] http://obs.carnegiescience.edu/Code/cosmos/

[30] IRAF is distributed by the National Optical Astronomy Observatory, which is operated by the Association of Universities for Research in Astronomy, Inc., under cooperative agreement with the National Science Foundation.

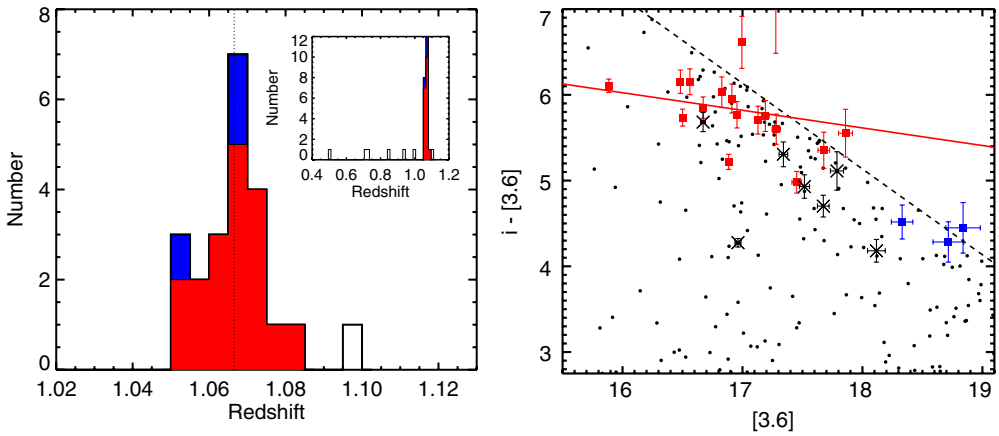

Figure 3. Left: histogram of spectroscopic redshifts obtained for SPT-CL J0546-5345, showing a very broad peak consisting of 21 members (shaded regions) centered at $\langle z \rangle = 1.0665$ (dotted line). The passive galaxies used in the dynamical analysis are shaded red. Galaxies for which redshifts were determined from [O II] emission are shaded blue. Spectroscopic non-members are unshaded. The inset shows all the secure redshifts obtained toward this cluster. Right: color–magnitude diagram in $i - [3.6]$ within a 2.′5 radius around SPT-CL J0546-5345. The red (blue) squares are the spectroscopically confirmed passive ([O II]) members. The passive members form a rich red sequence. Spectroscopic non-members are marked with X symbols. The 5σ color–magnitude limit is indicated by the dashed line. One member is omitted due to low-S/N photometry. The red line is the rest-frame Coma CMR, in the approximately $(U - H)$ color probed by our filters, normalized to match a BC03 passively evolving L^* galaxy.

(A color version of this figure is available in the online journal.)

Table 1
Spectroscopic Members of SPT-CL J0546-5345

ID	R.A. (J2000)	Decl. (J2000)	z	δz[a]	Principal Spectral Feature
J054637.2-534525	05:46:37.23	−53:45:25.6	1.0647	0.0002	Ca HK/D4000
J054636.2-534413	05:46:36.22	−53:44:13.4	1.0656	0.0004	Ca HK/D4000
J054642.3-534554	05:46:42.36	−53:45:54.5	1.0548	0.0003	Ca HK/D4000
J054633.6-534540	05:46:33.67	−53:45:40.5	1.0775	0.0005	Ca HK/D4000
J054635.1-534502	05:46:35.14	−53:45:02.0	1.0676	0.0003	Ca HK/D4000
J054638.9-534356	05:46:38.90	−53:43:56.2	1.0743	0.0003	Ca HK/D4000
J054634.8-534555	05:46:34.81	−53:45:55.6	1.0567	0.0002	Ca HK/D4000
J054635.8-534542	05:46:35.82	−53:45:42.0	1.0710	0.0003	Ca HK/D4000
J054638.6-534513	05:46:38.68	−53:45:13.7	1.0692	0.0003	Ca HK/D4000
J054644.3-534538	05:46:44.36	−53:45:38.4	1.0619	0.0002	Ca HK/D4000
J054645.0-534625	05:46:45.04	−53:46:25.9	1.0662	0.0003	Ca HK/D4000
J054641.8-534613	05:46:41.84	−53:46:13.5	1.0712	0.0004	Ca HK/D4000
J054630.3-534425	05:46:30.37	−53:44:25.3	1.0502	0.0005	Ca HK/D4000
J054638.8-534620	05:46:38.80	−53:46:20.2	1.0681	0.0004	Ca HK/D4000
J054633.8-534409	05:46:33.86	−53:44:09.3	1.0586	0.0005	Ca HK/D4000
J054646.8-534610	05:46:46.89	−53:46:10.9	1.0625	0.0005	Ca HK/D4000
J054634.9-534437	05:46:34.92	−53:44:37.5	1.0705	0.0005	Ca HK/D4000
J054636.4-534619	05:46:36.43	−53:46:19.5	1.0805	0.0007	Ca HK/D4000
J054644.4-534502	05:46:44.42	−53:45:02.7	1.0661	0.0025	[O II]
J054646.8-534557	05:46:46.87	−53:45:57.6	1.0686	0.0002	[O II]
J054642.0-534543	05:46:42.08	−53:45:43.9	1.0524	0.0002	[O II]

Note. [a] Redshift errors are twice those given by RVSAO.

errors (Danese et al. 1980). For the full membership, we find a mean redshift and velocity dispersion of $z = 1.0661^{+0.0018}_{-0.0022}$ and $\sigma = 1181^{+215}_{-186}$ km s^{-1}, respectively. The errors in both quantities, obtained from bootstrap resampling, represent the 68% confidence interval.

Since late-type members are often infalling, they tend to yield broader dispersions than early types (e.g., Girardi et al. 1996; Fadda et al. 1996; Mohr et al. 1996; Koranyi & Geller 2000). We therefore explore limiting our analysis to the 18 early-type members, as these are expected to better reflect the cluster potential. This approach yields nearly identical results, with a mean redshift of $z = 1.0665^{+0.0019}_{-0.0021}$ and a dispersion of $\sigma = 1179^{+232}_{-167}$ km s^{-1}. Although the biweight estimator is optimal, we also compute dispersions for these 18 members using both the gapper method (Beers et al. 1990) and the simple standard deviation. These yield $\sigma_{\rm gap} = 1170^{+240}_{-128}$ km s^{-1} and $\sigma_{\rm SD} = 1138^{+205}_{-132}$ km s^{-1}, respectively, both in excellent agreement with the biweight dispersion. There is no evidence of merger activity in SPT-CL J0546-5345 from the line-of-sight velocities, in either the appearance of Figure 3 or in the dispersion measures, although our redshift sampling is too sparse to rule it out.

Table 2
Comparison of Mass Measurements for SPT-CL J0546-5345

Mass Type	Proxy	Measurement	Units	Mass Scaling Relation	M_{200}[a,b] ($10^{14}\,M_\odot$)
Dispersion	**Biweight**	1179^{+232}_{-167}	km s^{-1}	σ–M_{200}(Evrard et al. 2008)	$\mathbf{10.4^{+6.1}_{-4.4}}$
	Gapper	1170^{+240}_{-128}	km s^{-1}	σ–M_{200} (Evrard et al. 2008)	$10.1^{+6.2}_{-3.3}$
	Std deviation	1138^{+205}_{-132}	km s^{-1}	σ–M_{200} (Evrard et al. 2008)	$9.3^{+5.0}_{-3.2}$
X-ray	$\boldsymbol{Y_X}$	5.3 ± 1.0	$\times 10^{14}\,M_\odot$keV	Y_X–M_{500} (Vikhlinin et al. 2009)	$\mathbf{8.23 \pm 1.21}$
	T_X	$7.5^{+1.7}_{-1.1}$	keV	T_X–M_{500} (Vikhlinin et al. 2009)	8.11 ± 1.89
SZE	$\boldsymbol{Y_{SZ}}$	3.5 ± 0.6	$\times 10^{14}\,M_\odot$keV	Y_{SZ}–M_{500} (A10)	$\mathbf{7.19 \pm 1.51}$
	S/N at 150 GHz	7.69		ξ–M_{500} (V10)	$5.03 \pm 1.13 \pm 0.77$
Richness	N_{200}	80 ± 31	Galaxies	N_{200}–M_{200} (H10)	$\mathbf{8.5 \pm 5.7 \pm 2.5}$
	N_{gal}	66 ± 7	Galaxies	N_{gal}–M_{200} (H10)	$9.2 \pm 4.9 \pm 2.7$
Best	**Combined**				$\mathbf{7.95 \pm 0.92}$

Notes.
[a] M_{500} masses were scaled to M_{200} masses assuming an NFW density profile and the mass-concentration relation of Duffy et al. (2008).
[b] We do not correct the dynamical masses for the small potential bias in the dispersion discussed in Section 3.4.

3.3. Color–Magnitude Relation

We plot the $i - [3.6]$ color–magnitude diagram for galaxies within a 2.′5 (1.22 Mpc) radius of SPT-CL J0546-5345 in Figure 3 (right). The spectroscopically confirmed passive galaxies define a rich red sequence, indicative of a cluster that is already well evolved at $z = 1.067$. The dashed line indicates the 5σ color–magnitude limit; one confirmed member is not detected robustly enough in the optical for inclusion in this plot. The solid red line indicates the slope of the rest-frame color–magnitude relation (CMR) of Coma (Eisenhardt et al. 2007), normalized to L^* at 3.6 μm in the passively evolving $z_f = 3$ BC03 model described above.

3.4. Dynamical Mass

There are several approaches in the literature for calculating the dynamical mass. Perhaps the most widely adopted is that of Carlberg et al. (1997), who use the simple definition $M_{200} = 4/3\,\pi\, r_{200}^3\, 200\,\rho_c$, where $r_{200} = \sqrt{3}\,\sigma/10\,H(z)$ and ρ_c is the critical density. Although this approach provides a convenient basis for comparison with other studies, it relies on the simplifying assumption that clusters are singular isothermal spheres. We therefore prefer to use the simulation-based σ–M_{200} relation of Evrard et al. (2008),

$$M_{200} = \frac{10^{15}}{h(z)} \left(\frac{\sigma_{\rm DM}}{\sigma_{\rm DM,15}} \right)^{1/\alpha}, \quad (1)$$

where $\sigma_{\rm DM,15} = 1082.9$ km s^{-1}, $\alpha = 0.3361$, and $\sigma_{\rm DM}$, the dark matter velocity dispersion, is related to the observed galaxy velocity dispersion by the velocity bias parameter, $b_v \equiv \sigma/\sigma_{\rm DM}$. Simulations generally suggest that $0.9 < b_v < 1.1$, and the most recent numerical results (Evrard et al. 2008, and references therein) indicate that galaxies are essentially unbiased tracers of the dark matter potential (i.e., $b_v = 1$). Adopting this value, we obtain $M_{200} = 1.04^{+0.61}_{-0.44} \times 10^{15}\,M_\odot$. Dynamical masses corresponding to the various velocity dispersion measures reported in Section 3.2 are tabulated in Table 2. The Carlberg et al. (1997) relation yields masses a factor of $\approx$1.5 larger.

Detailed studies of the velocity dispersion profile (e.g., Girardi et al. 1993; Fadda et al. 1996) indicate that dispersions measured within radii less than r_{200} may be biased high. In A10, r_{200} for SPT-CL J0546-5345 is estimated to be $\approx$ 1.57 Mpc, and we are therefore probing an aperture of $\approx 0.57 r_{200}$. Numerical (Biviano et al. 2006) and observational (Rines & Diaferio 2006; Katgert et al. 1996, 1998) studies suggest that for our early-type galaxy sample and the clustercentric radius probed, the bias is expected to be small. For example, Biviano et al. (2006) report the expected bias in the dispersion as a function of the fractional virial radius probed; for our dispersion measurement the expected upward bias is $\lesssim$2.5%. This implies a corresponding bias in the dynamical mass of $\lesssim$7%, which would lower the dynamical mass to $\sim 9.6 \times 10^{14}\,M_\odot$. While this may well be a more accurate value, the bias correction is both uncertain and small. We therefore defer a more extensive analysis to a future paper, when a larger sample of spectroscopic members out to r_{200} is available.

Finally, we note that no other $z > 1$ cluster with $\geqslant$10 spectroscopically confirmed members has $\sigma > 1000$ km s^{-1}. With a dispersion of $\sigma = 1179$ km s^{-1}, SPT-CL J0546-5345 is unambiguously the most dynamically massive cluster yet identified at $z > 1$.

4. DISCUSSION

4.1. σ–T_X Relation

At $T_X = 7.5^{+1.7}_{-1.1}$ keV, SPT-CL J0546-5345 is among the hottest clusters yet observed in the X-ray at $z > 1$ (Rosati et al. 2009). Figure 4 shows the well-known correlation between X-ray temperature and galaxy velocity dispersion (Lubin & Bahcall 1993; Bird et al. 1995; Girardi et al. 1996; Horner et al. 1999; Xue & Wu 2000; Ortiz-Gil et al. 2004). The clusters shown are the subset of the well-studied, low-redshift X-ray cluster sample of Vikhlinin et al. (2009) for which accurate velocity dispersion measurements, from at least 40 galaxies, are available from Girardi et al. (1996). The temperatures are measured in an identical manner to that of SPT-CL J0546-5345, which is plotted as the large red circle. The dashed line is the best-fit relation Girardi et al. (1996) obtained using previous temperatures from the literature, and the solid line is our own fit using the Vikhlinin et al. (2009) temperatures. Both fits exclude SPT-CL J0546-5345, and are consistent with typical measurements (e.g., Lubin & Bahcall 1993; Horner et al. 1999). Although the comparison clusters are all at low redshift ($z < 0.1$), there is no expectation of, nor evidence for, evolution in this relation to $z \sim 1$ (e.g., Wu et al. 1998; Tran et al. 1999). The measured dispersion

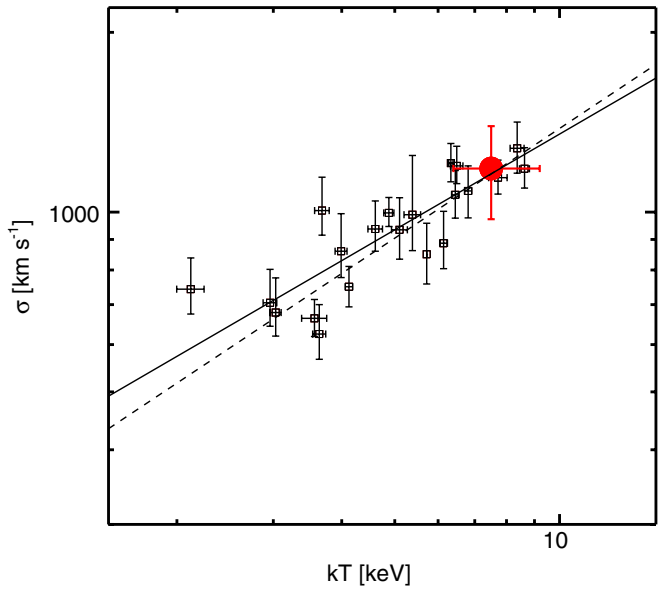

Figure 4. Empirical σ–T_X correlation for the X-ray clusters from Vikhlinin et al. (2009), with velocity dispersions taken from Girardi et al. (1996). The temperatures are measured exactly as for SPT-CL J0546-5345. The fits, described in the text, are typical of those found by other authors (e.g., Lubin & Bahcall 1993; Horner et al. 1999). SPT-CL J0546-5345 (red circle) falls right on this relation.

and X-ray temperature for SPT-CL J0546-5345 fall right on the σ–T_X relation, offering strong corroboration of the very large dynamical mass presented here.

4.2. X-ray, SZE, and Optical Mass Measures

We now compare the dynamical mass with several other mass measures available for SPT-CL J0546-5345, all reported in terms of $M_{200}(\rho_c)$. A summary of these mass measures is given in Table 2.

In A10, the cluster mass within r_{500} is measured using the Y_X–M_{500} relation (Vikhlinin et al. 2009) to be $M_{500,\mathrm{Y_X}} = (5.33 \pm 0.62) \times 10^{14}\,M_\odot$. The systematic uncertainty of this scaling relation calibration was estimated by Vikhlinin et al. (2009) to be ±9% by comparing X-ray mass estimates to weak lensing mass measurements for a representative sample of clusters. We include this uncertainty in quadrature when converting to $M_{200,\mathrm{Y_X}}$, and we estimate that $M_{200,\mathrm{Y_X}} = (8.23 \pm 1.21) \times 10^{14}\,M_\odot$. This X-ray mass is consistent with the measured dynamical mass within the errors. Although the X-ray image shows evidence of a possible merger, the Y_X estimator is expected to be robust to such events (Vikhlinin et al. 2009). Indeed, the majority of high-redshift clusters have asymmetrical X-ray morphologies (e.g., Vikhlinin et al. 2009; A10), so the inferred X-ray mass of SPT-CL J0546-5345 should be of comparable accuracy to other clusters at similar redshifts. We also estimate the mass from the temperature, via the T_X–M_{500} relation of Vikhlinin et al. (2009), to be $M_{200,\mathrm{T_X}} = (8.11 \pm 1.89) \times 10^{14} M_\odot$.

The SZE measurement of the integrated Comptonization, Y_{SZ}, is expected to be the most accurate Sunyaev–Zel'dovich (SZ) mass proxy (Motl et al. 2005; Nagai 2006). In A10, they measure a spherically deprojected Comptonization of $Y_{\mathrm{SZ}} = (3.5 \pm 0.6) \times 10^{14}\,M_\odot$keV, where the uncertainty is estimated from the quadrature sum of statistical errors and the uncertainty in the assumed gas profile. From this measurement, we use the Y_{SZ}–M_{500} relation reported in A10 to estimate a mass, where we marginalize over the allowed range of normalization and slope parameters from their fit. We include an additional ±9% uncertainty to account for the systematic uncertainty of the Y_X-based masses used to calibrate their relation.[31] Using this method, we infer a mass of $M_{200,\mathrm{Y_{SZ}}} = (7.19 \pm 1.51) \times 10^{14}\,M_\odot$, in agreement with the X-ray and dynamical mass estimates.

Another SZ mass estimate can be inferred from the SZE significance-mass scaling relation established via WMAP7-constrained simulations in V10. A10 compared this SZE significance-based mass proxy with X-ray-inferred masses for their sample of 15 SZE-selected clusters, finding that the significance-based SZE masses may be biased low, with an average ratio of the SZE to X-ray masses of 0.89 ± 0.06. The result for SPT-CL J0546-5345, $M_{200,\mathrm{SZ}} = (5.03 \pm 1.13 \pm 0.77) \times 10^{14}\,M_\odot$, where the uncertainties are statistical followed by systematic, is indeed $\sim 1.6\sigma$ below the 68% confidence interval of the more precise X-ray mass, although it is in agreement with the dynamical mass within the errors. Accounting for the bias quantified in A10 brings the significance-based mass estimate into agreement with the X-ray mass.

H10 present a scaling relation between SZE-derived mass and two optical richness measures, N_{gal} and N_{200}. These richness measures count the number of galaxies on the red sequence at the cluster redshift within clustercentric radii of $1\ h^{-1}$ Mpc and r_{200}, respectively. The derived masses, $M_{200}(N_{\mathrm{gal}}) = (9.2 \pm 4.9 \pm 2.7) \times 10^{14}\,M_\odot$ and $M_{200}(N_{200}) = (8.5 \pm 5.7 \pm 2.5) \times 10^{14}\,M_\odot$, are consistent with the independent richness-based mass estimate of Menanteau & Hughes (2009) for this cluster. Although noisy mass proxies, these richness measures offer independent evidence of the high mass of SPT-CL J0546-5345.

4.3. Combined Mass for SPT-CL J0546-5345

Table 2 lists total mass measures for SPT-CL J0546-5345 from dynamical, X-ray, SZE, and optical richness mass proxies. For each physical probe, the bold entries indicate the specific proxy expected to yield the most robust mass. For dispersions, this is the biweight measure, which is optimal for the number of spectroscopic members we have (Beers et al. 1990). For the X-ray, the Y_X estimator is chosen over the T_X estimator because it is expected to be significantly less biased for mergers and to have less intrinsic scatter with mass (Kravtsov et al. 2006; Vikhlinin et al. 2009). For the SZE, the Y_{SZ} estimator is chosen over the S/N estimator because its scaling relations have been calibrated directly from external observations rather than simulations and it is expected to have less intrinsic scatter with mass (Kravtsov et al. 2006; V10). Finally, the N_{200} estimator is the best-tested optical richness measure.

We optimally combine these independent measurements, weighting them by their errors. We symmetrize the errors on the dynamical mass and add the statistical and systematic errors in quadrature for the richness. The combined mass is insensitive to these details since these are the least constrained measures. The resulting mass is $M_{200} = (7.95 \pm 0.92) \times 10^{14}\,M_\odot$, which we take as our best estimate of the mass of SPT-CL J0546-5345.

[31] The SZ and X-ray mass estimates are not completely independent. We expect that their largest correlation will be from the mass calibration of the Y_X–M_{500} and Y_{SZ}–M_{500} relations, which are based on the same X-ray measurements from Vikhlinin et al. (2009). We add the 9% uncertainty to the Y_{SZ} mass estimate to account for this, and assume that any other correlated uncertainty is negligible.

4.4. SPT-CL J0546-5345 in a Cosmological Context

Using the Tinker et al. (2008) mass function we calculate that SPT-CL J0546-5345, which at $z = 1.067$ is already almost as massive as the Coma cluster, will increase in mass by a factor of ∼4 over the next 8 Gyr. It should therefore grow into one of the most massive clusters in the universe by the present day.

Historically, the existence of individual massive galaxy clusters at high redshift has been used to constrain cosmological models (e.g., Donahue et al. 1998). While we are entering an era where large samples of SZ clusters will soon be available in addressing such questions, it is interesting to ask whether the existence of SPT-CL J0546-5345 is expected in our survey volume for a concordance ΛCDM cosmology. Convolving the Tinker et al. (2008) mass function with a Gaussian mass probability function for the best-estimate mass of SPT-CL J0546-5345, we find that ΛCDM predicts the existence of 0.18 clusters of this mass or higher at $z > 1$ in 178 deg^2. We note that the M_{500}–Y_X relation was calibrated at lower redshifts ($z \lesssim 0.6$) than SPT-CL J0546-5345, and the accuracy of this relation has not been verified at $z \gtrsim 1$. Given the caveats and uncertainties inherent in this calculation, we conclude that the existence of SPT-CL J0546-5345 in our survey volume is unsurprising. The complete SPT sample, combined with improved mass scaling relations based on complementary mass measures, will permit ΛCDM predictions for the high end of the cluster mass function to be robustly tested at high redshift.

5. CONCLUSIONS

We report the spectroscopic confirmation SPT-CL J0546-5345 at $z = 1.067$, the first SZE-selected galaxy cluster at $z > 1$. We measure a robust velocity dispersion from 18 early-type members of $\sigma = 1179^{+232}_{-167}$ km s^{-1}, corresponding to a dynamical mass of $M_{200} = 1.0^{+0.6}_{-0.4} \times 10^{15}\, M_\odot$. SPT-CL J0546-5345 is the most dynamically massive cluster yet identified, from any method, at $z > 1$.

We find excellent consistency across several independent mass measures. The measured dispersion and X-ray temperature of SPT-CL J0546-5345 fall right on the σ–T_X relation. The X-ray, SZE, and richness-based mass estimates are all consistent with the dynamical mass, and with each other, within the errors. Combining all the mass measures, we derive a best-estimate mass for SPT-CL J0546-5345 of $M_{200} = (7.95 \pm 0.92) \times 10^{14}\, M_\odot$.

In ΛCDM, we expect 0.18 clusters consistent with this mass above $z > 1$ in our survey area. Given the uncertainties in X-ray scaling relations at high redshift, we conclude that the existence of SPT-CL J0546-5345 in our survey volume is unsurprising. The complete SPT sample will provide the large sample of clusters required to robustly test the high redshift, high mass end of the cluster mass function.

The SPT is supported by the National Science Foundation through grant ANT-0638937. Partial support is also provided by the NSF Physics Frontier Center grant PHY-0114422 to the Kavli Institute of Cosmological Physics at the University of Chicago, the Kavli Foundation, and the Gordon and Betty Moore Foundation. This work is based in part on observations made with the *Spitzer Space Telescope*, which is operated by the Jet Propulsion Laboratory, California Institute of Technology under a contract with NASA. Support for this work was provided by NASA through an award issued by JPL/Caltech. This paper includes data gathered with the 6.5 meter Magellan Telescopes located at Las Campanas Observatory, Chile. This work is based in part on observations obtained with the *Chandra X-ray Observatory*, under contract SV4-74018, A31 with the Smithsonian Astrophysical Observatory which operates the *Chandra* for NASA. We are very grateful for the efforts of the *Spitzer*, *Chandra*, Magellan, and CTIO support staff without whom this paper would not be possible. Support for M.B. was provided by the W. M. Keck Foundation. B.S. acknowledges support from the Brinson Foundation.

REFERENCES

Andersson, K., et al. 2010, ApJ, submitted (arXiv:1003.3068)
Ashby, M. L. N., et al. 2009, ApJ, 701, 428
Beers, T. C., Flynn, K., & Gebhardt, K. 1990, AJ, 100, 32
Bird, C. M., Mushotzky, R. F., & Metzler, C. A. 1995, ApJ, 453, 40
Biviano, A., Murante, G., Borgani, S., Diaferio, A., Dolag, K., & Girardi, M. 2006, A&A, 456, 23
Brodwin, M., et al. 2006, ApJ, 651, 791
Bruzual, G., & Charlot, S. 2003, MNRAS, 344, 1000
Carlberg, R. G., Yee, H. K. C., & Ellingson, E. 1997, ApJ, 478, 462
Carlstrom, J. E., Holder, G. P., & Reese, E. D. 2002, ARA&A, 40, 643
Carlstrom, J. E., et al. 2009, PASP, submitted (arXiv:0907.4445)
Cavaliere, A., & Fusco-Femiano, R. 1978, A&A, 70, 677
Danese, L., de Zotti, G., & di Tullio, G. 1980, A&A, 82, 322
Donahue, M., Voit, G. M., Gioia, I., Lupino, G., Hughes, J. P., & Stocke, J. T. 1998, ApJ, 502, 550
Dressler, A., Hare, T., Bigelow, B. C., & Osip, D. J. 2006, Proc. SPIE, 6269, 13
Duffy, A. R., Schaye, J., Kay, S. T., & Dalla Vecchia, C. 2008, MNRAS, 390, L64
Dunkley, J., et al. 2009, ApJS, 180, 306
Eisenhardt, P. R., De Propris, R., Gonzalez, A. H., Stanford, S. A., Wang, M., & Dickinson, M. 2007, ApJS, 169, 225
Eisenhardt, P. R. M., et al. 2008, ApJ, 684, 905
Elston, R. J., et al. 2006, ApJ, 639, 816
Evrard, A. E., et al. 2008, ApJ, 672, 122
Fadda, D., Girardi, M., Giuricin, G., Mardirossian, F., & Mezzetti, M. 1996, ApJ, 473, 670
Foley, R. J., et al. 2003, PASP, 115, 1220
Fowler, J. W., et al. 2007, Appl. Opt., 46, 3444
Girardi, M., Biviano, A., Giuricin, G., Mardirossian, F., & Mezzetti, M. 1993, ApJ, 404, 38
Girardi, M., Fadda, D., Giuricin, G., Mardirossian, F., Mezzetti, M., & Biviano, A. 1996, ApJ, 457, 61
Gladders, M. D., & Yee, H. K. C. 2005, ApJS, 157, 1
High, F. W., Stubbs, C. W., Rest, A., Stalder, B., & Challis, P. 2009, AJ, 138, 110
High, F. W., et al. 2010, ApJ, submitted (arXiv:1003.0005)
Horner, D. J., Mushotzky, R. F., & Scharf, C. A. 1999, ApJ, 520, 78
Katgert, P., Mazure, A., den Hartog, R., Adami, C., Biviano, A., & Perea, J. 1998, A&AS, 129, 399
Katgert, P., et al. 1996, A&A, 310, 8
Koranyi, D. M., & Geller, M. J. 2000, AJ, 119, 44
Kravtsov, A. V., Vikhlinin, A., & Nagai, D. 2006, ApJ, 650, 128
Kurtz, M. J., & Mink, D. J. 1998, PASP, 110, 934
Lubin, L. M., & Bahcall, N. A. 1993, ApJ, 415, L17
Menanteau, F., & Hughes, J. P. 2009, ApJ, 694, L136
Mohr, J. J., Geller, M. J., Fabricant, D. G., Wegner, G., Thorstensen, J., & Richstone, D. O. 1996, ApJ, 470, 724
Mohr, J. J., et al. 2008, Proc. SPIE, 7016, 17
Motl, P. M., Hallman, E. J., Burns, J. O., & Norman, M. L. 2005, ApJ, 623, L63
Mullis, C. R., Rosati, P., Lamer, G., Böhringer, H., Schwope, A., Schuecker, P., & Fassbender, R. 2005, ApJ, 623, L85
Muzzin, A., et al. 2009, ApJ, 698, 1934
Nagai, D. 2006, ApJ, 650, 538
Ngeow, C. C., Mohr, J., Zenteno, A., Data Management, D., BCS, & SPT Collaborations 2009, BAAS, 41, 335
Ortiz-Gil, A., Guzzo, L., Schuecker, P., Böhringer, H., & Collins, C. A. 2004, MNRAS, 348, 325
Papovich, C., et al. 2010, ApJ, 716, 1503
Quintana, H., Carrasco, E. R., & Reisenegger, A. 2000, AJ, 120, 511
Rines, K., & Diaferio, A. 2006, AJ, 132, 1275
Rosati, P., et al. 2004, AJ, 127, 230
Rosati, P., et al. 2009, A&A, 508, 583

Stanford, S. A., Elston, R., Eisenhardt, P. R., Spinrad, H., Stern, D., & Dey, A. 1997, AJ, 114, 2232
Stanford, S. A., et al. 2006, ApJ, 646, L13
Staniszewski, Z., et al. 2009, ApJ, 701, 32
Sunyaev, R. A., & Zel'dovich, Y. B. 1972, Comments Astrophys. Space Phys., 4, 173
Tinker, J., Kravtsov, A. V., Klypin, A., Abazajian, K., Warren, M., Yepes, G., Gottlöber, S., & Holz, D. E. 2008, ApJ, 688, 709
Tran, K., Kelson, D. D., van Dokkum, P., Franx, M., Illingworth, G. D., & Magee, D. 1999, ApJ, 522, 39
Vanderlinde, K., et al. 2010, ApJ, in press (arXiv:1003.0003)
Vikhlinin, A., Kravtsov, A., Forman, W., Jones, C., Markevitch, M., Murray, S. S., & Van Speybroeck, L. 2006, ApJ, 640, 691
Vikhlinin, A., et al. 2009, ApJ, 692, 1033
Wu, X., Chiueh, T., Fang, L., & Xue, Y. 1998, MNRAS, 301, 861
Xue, Y., & Wu, X. 2000, ApJ, 538, 65